The quantum taste of hydrogen

Philippe Depondt, Simon Huppert, Fabio Finocchi

EPJ Web of Conferences **263**, 01014 (2022) https://doi.org/10.1051/epjconf/202226301014
8th Complexity-Disorder Days 2021

The quantum taste of hydrogen.

At the borderline between classical and quantum physics.

Philippe Depondt[1,*], *Simon* Huppert[1,**], and *Fabio* Finocchi[1,***]

[1]Institut des NanoSciences de Paris (INSP), Sorbonne Université, CNRS-UMR 7588, 75005 Paris, France

Abstract. Electronic properties of materials are dominated by quantum effects, but nuclei, being much heavier, are usually treated as classical particles. This approximation, although tremendously convenient, is not always valid, even in close to ambient pressure and temperature conditions, especially when light nuclei such as hydrogen are involved. Zero point energy and proton tunneling can be relevant. Isotopic effects, obtained by replacing hydrogen with deuterium, are observed experimentally and are a clear indication of Nuclear Quantum Effects (NQE) since mean values obtained through classical statistical physics do not depend on mass. Introducing NQEs into simulations at an acceptable computational cost raises fundamental questions and yields subtle and unexpected results.

1 Introduction

Atomic nuclei are relatively heavy with respect to electrons, and therefore usually considered as classical particles. However they are sometimes at the border at which their "quantumness" cannot be completely neglected. The introduction of quantum physics, even when relatively moderate, generates effects that are both complex and subtle, and largely escape intuition.

It has been well known for almost a century that heavy water, in which the hydrogen atoms of H_2O are substituted with their isotope deuterium D, the same chemical but twice heavier, is toxic (see e.g. [1]): since its discovery in 1932, numerous experiments were carried out with bacteria, fungi, algæ, plants, fish, frogs and mice (albeit *not*, to our knowledge, with human beings)... High concentrations (up to 92%) of D_2O will eventually kill many living organisms. It seems that D_2O will interfere with the cell division process with dramatic consequences on life.

As the chemical properties of H_2O and D_2O are exactly the same, this raises a question: why should a simple change of the mass of an atom, with no alteration of its electronic structure, which is the basis for its chemical properties, have such consequences?

Of course, it is also well known that the melting point of deuterated water is 3.8°C instead of 0°C, while boiling takes place at 101°C instead of 100°C. More spectacular, the ice-VII to ice-X structural phase transition at room temperature under high pressure occurs at 65GPa for H_2O [2–6] and approximately 90 GPa for D_2O [7, 8].

Many other such examples exist: for instance KOH and KOD [9] exhibit a 30K temperature difference for a structural phase transition at ambient pressure; NaOH is paraelectric without change as temperature is decreased, while NaOD undergoes a phase transition to an antiferroelectric structure at 150K [10–13]. $SrTiO_3$ also shows isotopic effects [14] upon O^{16}-O^{18} substitution.

Changes in the chemical bonds can hardly be invoked for these behaviors while the evaluation of mean values of observables such as lattice constants, structure, etc., via classical statistical physics is not sensitive to mass. One should therefore take into account the quantum behavior, not only of the electrons, but also of the nuclei. Introducing quantum mechanics into molecular dynamics simulations is by no means trivial and we attempt to show in this paper how it can be done.

We therefore recall in section 2 some relevant ideas about molecular dynamics simulations, then, in section 3, we introduce general issues with nuclear quantum effects and briefly develop methods, successes and problems in section 4.

2 Molecular dynamics simulations

Condensed matter physicists deal with systems that contain a large number of atoms (Avogadro's number which gives an indication of the number of atoms in a macroscopic sample weighing a few grams is tremendous: $\mathcal{A} = 6.02 \times 10^{23}$) so that trying explicitly to solve the related equations is absolutely out of reach. It turns out that, in many cases, using a computer to solve these equations for a few hundreds of atoms is quite enough accurately to evaluate the quantities of interest, compare with experimental results, etc. Large efforts are devoted to such simulations, as they are often the key to understanding the underlying mechanisms behind observable effects and properties of considerable practical importance for many materials of interest.

*e-mail: philippe.depondt@sorbonne-universite.fr
**e-mail: simon.huppert@sorbonne-universite.fr
***e-mail: fabio.finocchi@sorbonne-universite.fr

Several additional approximations are also usually made:

- the so-called Born-Oppenheimer approximation [15]: electrons are about 2000 times lighter than the lightest nucleus (hydrogen) and therefore can be considered to react almost instantly to nuclear motion and always be at equilibrium with the nuclear configuration,
- the electronic structures cannot be calculated exactly, however the "Density Functional Theory" (DFT) [16, 17] allows to evaluate with reasonable accuracy atom-atom interactions,
- since the above approximation provides the forces between atoms, it is possible numerically to integrate Newton's classical equations of motion: *this approximation assumes the nuclei to be heavy enough to be considered as classical particles*: their quantum behavior is ignored.

While numerous very precise and highly informative such simulations were done over the years, and continue to provide invaluable insights into the behavior of many systems, it is this last assumption, using Newton's *classical* equations, that is being seriously questioned by the examples mentioned in the introduction (section 1). These examples show that, in some cases, especially when hydrogen is involved (which is quite often!), quantum corrections should somehow be included into our simulations.

3 Nuclear quantum effects (NQE).

3.1 Classical statistical physics will not work!

When a large number of particles is involved, physicists use statistics to compute the mean values of the quantities they are interested in, instead of trying to keep track of all the details of the individual adventures of every particle. These mean values are obtained by summing on the positions and velocities of all the particles in the system. Assume we are interested in quantity a (for instance, say, the average distance between two atoms, or the angle between two bonds): the mean value of a, denoted $\langle a \rangle$ writes:

$$\langle a \rangle = \frac{\int a(\mathbf{r},\mathbf{p})\, \mathrm{e}^{-\frac{\mathbf{p}^2/2m+V(\mathbf{r})}{k_B T}} d\mathbf{r}\, d\mathbf{p}}{\int \mathrm{e}^{-\frac{\mathbf{p}^2/2m+V(\mathbf{r})}{k_B T}} d\mathbf{r}\, d\mathbf{p}} \tag{1}$$

where $\mathbf{r}$, $\mathbf{p}$ and m are the positions, momenta and mass of the particles, $V(\mathbf{r})$ the potential energy of the system, T the temperature and k_B Boltzmann's constant. Equation (1) states that the mean value of a is the integral of a over position and momentum (that is: all accessible states) weighed by the probability of each state $(\mathbf{r}, \mathbf{p})$. In *classical* statistical physics, if a does not depend on momentum (or velocity), the integrals over $\mathbf{p}$, on numerator and denominator, cancel out and yield:

$$\langle a \rangle = \frac{\int a(\mathbf{r})\, \mathrm{e}^{-\frac{V(\mathbf{r})}{k_B T}} d\mathbf{r}}{\int \mathrm{e}^{-\frac{V(\mathbf{r})}{k_B T}} d\mathbf{r}} \tag{2}$$

This simply states that mass vanishes from the expression in equation (2): therefore *substituting hydrogen with deuterium will only increase mass and not change the mean value of any velocity-independent observable in the system*: vibrational frequencies will change because deuterium is heavier, but structural properties should not be altered, in contradiction with what the examples in section 1 tend to show.

In order to re-insert mass into these averages, one may first note that equations (1) are (2) are not valid in a quantum physics framework (technically because, then, $\mathbf{r}$ and $\mathbf{p}$ are not numbers but non-commuting operators). More generally, quantum physics states that a particle is not precisely localized in space, and an estimate of this quantum delocalization is given, for a free particle, by de Broglie's thermal wavelength :

$$\lambda_{dB} = \sqrt{\frac{2\pi\hbar^2}{m\, k_B T}} \tag{3}$$

which does depend on the mass m, $\hbar$ being Planck's reduced constant. The following orders of magnitude are of interest: for hydrogen at room temperature $\lambda_{dB} \approx 1$Å, while for deuterium $\lambda_{dB} \approx 0.7$ Å, which can be compared with the O−H covalent bond length $d_{\mathrm{OH}} \approx 1$ Å in many compounds. The de Broglie wavelength difference between the two isotopes is not negligible with respect to the OH bond length, and therefore, this latter point should lead us into introducing into models quantum effects, for at least light nuclei which can be significantly delocalized. In practice, the problem is more complicated than suggested by equation (3), since the particles under study are not free but interacting with others, so that the actual quantum effects have to be examined for each physical system specifically.

3.2 The textbook case of high-pressure ice: from ice VII to ice X.

Before going into technical points, it is worth trying to understand, at least qualitatively, what is happening in high-pressure ice (for a detailed description, see [8] and references therein) and how quantum delocalization can alter a phase transition, for instance.

At room temperature and $5 < P < 65$ GPa, the stable phase of water is ice-VII, a body-centered cubic (bcc) structure with an oxygen atom on each corner of the cube and one at the center (figure 1). The hydrogen atoms are located on the diagonals of the cube between the oxygen atoms, but they are not at the mid-point between oxygens: they are bonded to one oxygen atom via a short (≈ 1 Å) covalent bond and to the other through a longer (≈ 1.5-2 Å) and much weaker hydrogen bond. It is worth mentioning however that most of the intriguing properties of water are *in fine* determined by this longer hydrogen bond.

In practice, the hydrogen atom is caught in a double-well potential and will rest in one of the wells.

When pressure is increased, the oxygen atoms are pushed closer (figure 2): the covalent O−H bond, being very strong, does not change much, so it is the hydrogen bond length that is decreased significantly. From an energy viewpoint (figure 3), the two wells move closer while

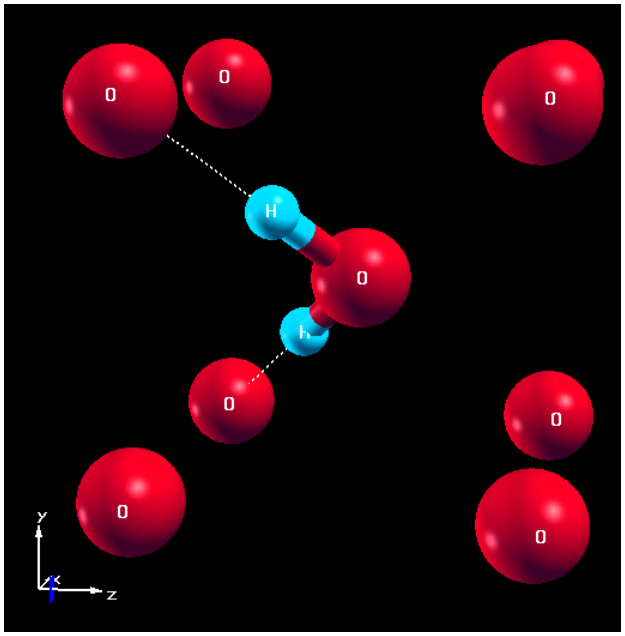

Figure 1. The structure of ice VII for pressures $P < 65$ GPa. Oxygen atoms (in red) form a body-centered cube, while the hydrogen atoms (light blue) are located between the oxygen atoms in an asymmetric position. The thin dashed lines represent weak hydrogen bonds, while the bond with the nearest oxygen atom is covalent. Each oxygen atom has 2 hydrogen neighbours (only 2 are represented on the figure, the others associated with the other oxygen atoms have been omitted for clarity).

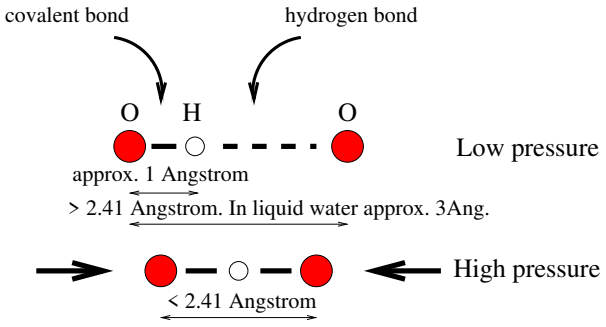

Figure 2. Location of the hydrogen atoms between oxygen atoms in an asymmetric position for ice VII at low pressure (top) and in a symmetric position for ice X at high pressure (bottom) when the oxygen atoms are pushed closer with $d_{O-O} < 2.41$Å.

the barrier height decreases. When the barrier vanishes at high enough a pressure, the structure changes to ice X and the hydrogen atom will sit in the middle: this is called a "symmetrization" transition. There is no "quantumness" involved in this explanation, and indeed this transition can occur within a classical frame, but only around 90 to 100 GPa instead of 65! We still have an error of approximately 30 GPa, which is by no means negligible.

Now, if the hydrogen atom is significantly delocalized as can be inferred from the end of section 3.1, it will explore the potential well in which it is lying, even when the temperature equals zero (figure 4). The result will be that its energy will be greater than the potential minimum: this

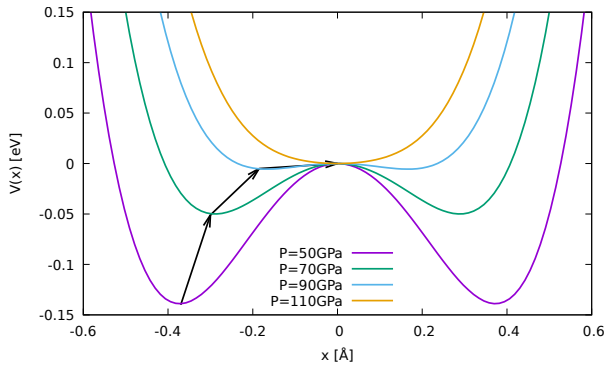

Figure 3. Potential energy of the system as a function of the hydrogen atom position x between its two neighbouring oxygen atoms for several pressures. The transition mechanism for ice is shown from a classical viewpoint: as pressure is increased, the two potential wells move closer and the barrier eventually vanishes.

is called Zero-Point Energy (ZPE). The hydrogen atom will thus be able to cross the energy barrier before it vanishes, therefore at a lower pressure than initially expected. In many systems, this happens when the O−O distance becomes less than approximately 2.41Å.

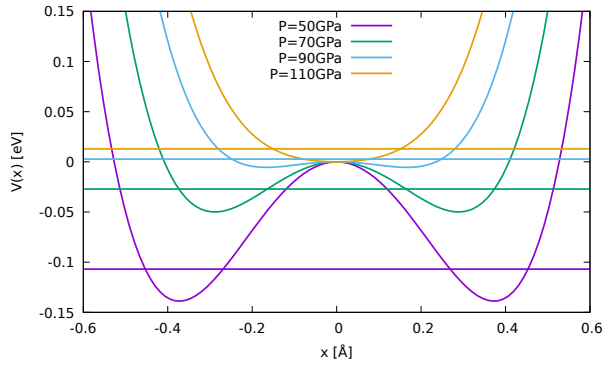

Figure 4. Transition mechanism in ice from a quantum viewpoint: the horizontal lines (colors correspond to the potential energy curve at the same pressure) represent the minimum energy for each pressure increased with the zero-point energy showing how the effective barrier is decreased, which allows the transition at a lower pressure than in the classical case (figure 3).

The most striking effect of the ZPE is therefore a significant reduction of the transition pressure.

3.3 Why quantum physics is in practice intractable: exponential divergence

It therefore appears that NQEs should be included, when relevant, into simulations. The most straightforward approach to quantum dynamics is Schrödinger's time-dependent equation:

$$i\hbar\frac{\partial\psi(\mathbf{r},t)}{\partial t} = -\frac{\hbar^2}{2m}\Delta_{\mathbf{r}}\psi(\mathbf{r},t) + V(\mathbf{r})\,\psi(\mathbf{r},t) \qquad (4)$$

The trouble with equation (4) is that the wave-function $\psi(\mathbf{r}, t)$, the unknown function that is the solution of the equation, is a function of t but also of $\mathbf{r}$, a vector that contains the coordinates of all the particles that are part of the system under scrutiny. This means that ψ is an extraordinarily complicated function of a tremendous number of coordinates.

Equation (4) can indeed be solved for a small number of degrees of freedom, but for a reasonable number from a condensed matter physicist's point of view (maybe 300 degrees of freedom for one hundred particles, and over a duration of 20×10^{-12}s), the computational power of the largest computer in the world would be orders of magnitude below what is needed.

Approximations must therefore be made.

4 Methods

Nuclei, including hydrogen, are much heavier than e.g. electrons so that, while introducing quantum effects, we shall mainly be interested in zero-point energy and relatively modest quantum delocalization: issues connected with exchange or interference will reasonably be left out, in most cases, without major damage.

Several approaches were developed in the past and are currently used. Path-integral (PI) based methods stem from Feynman's formalism [18] and mimic quantum delocalization by generating many trajectories with the correct distribution. Generalized Langevin (GL) based methods use a stochastic process for the same purpose. Both involve modified classical equations of motion. PI is often considered the reference method as it converges towards exact quantum distributions as the number of trajectories is increased with the drawback of rapidly increasing computational cost. GL is a somewhat more radical approximation as it has negligible additional computation cost as compared with classical molecular dynamics simulations.

4.1 Path-integral based methods

4.1.1 Splitting probabilities.

These methods are based on Feynman's general path-integral treatment of the partition function in a quantum system [18]. Following Barker's derivation [19], we start with the density operator at a given temperature T:

$$\rho = \mathrm{e}^{-\beta H} = \mathrm{e}^{-\beta\left(-\frac{\hbar^2}{2m}\sum_i \nabla_i^2 + V(\mathbf{r})\right)} \tag{5}$$

where $\beta = (k_B T)^{-1}$ is the inverse temperature, H the Hamiltonian operator and $V(\mathbf{r})$ the potential energy. Equation (5) yields the expression for the density matrix of the system (a key quantity from which time-independent expectation values at equilibrium can be derived) :

$$\rho(\mathbf{r}, \mathbf{r}'; \beta) = \sum_n \mathrm{e}^{-\beta E_n} \psi_n(\mathbf{r}) \psi_n^*(\mathbf{r}') \tag{6}$$

where E_n represents the eigen-energies as obtained from Schrödinger's stationary equation, and $\psi_n(\mathbf{r})$ the corresponding wave-functions. We need to evaluate ρ as, neglecting exchange, the partition function, which is the key to statistical mechanics, writes for a system of N particles:

$$Z = \frac{1}{N!} \int \rho(\mathbf{r}, \mathbf{r}; \beta)\, d\mathbf{r} \tag{7}$$

Equation (6) rewrites:

$$\rho(\mathbf{r}, \mathbf{r}'; \beta) =$$
$$\int \sum_n \mathrm{e}^{-\beta' E_n} \psi_n(\mathbf{r}) \psi_n^*(\mathbf{r}'') \sum_{n'} \mathrm{e}^{-(\beta-\beta')E_{n'}} \psi_{n'}(\mathbf{r}'') \psi_{n'}^*(\mathbf{r}')\, d\mathbf{r}''$$
$$= \int \rho(\mathbf{r}, \mathbf{r}''; \beta')\, \rho(\mathbf{r}'', \mathbf{r}'; \beta - \beta')\, d\mathbf{r}'' \tag{8}$$

This is true because the wave-functions are both orthogonal and normalized.

Equation (8) can be applied repeatedly, introducing many $\mathbf{r}''$ intermediates: $\mathbf{r}_1 \ldots \mathbf{r}_M$, and inverse temperature intermediates $\beta_1 \ldots \beta_M$ with $\beta_i - \beta_{i-1} = \beta/M$. What this means is that the integral in equation (7) can be expanded into small pieces $\mathbf{r}_1 \ldots \mathbf{r}_M, \beta_1 \ldots \beta_M$. If M is large enough, β/M can be considered small. Also, since, in equation (7), we need $\rho(\mathbf{r}, \mathbf{r}; \beta)$ (not $\rho(\mathbf{r}, \mathbf{r}'; \beta)$), we must have $\mathbf{r}_M = \mathbf{r}_1$. Thus, the integral in equation (7) for the partition function rewrites:

$$\int \rho(\mathbf{r}_1, \mathbf{r}_1; \beta)\, d\mathbf{r}_1 = \int \cdots \int$$
$$\rho(\mathbf{r}_1, \mathbf{r}_2; \frac{\beta}{M}) \ldots \rho(\mathbf{r}_{M-1}, \mathbf{r}_M; \frac{\beta}{M})\, \rho(\mathbf{r}_M, \mathbf{r}_1; \frac{\beta}{M})$$
$$d\mathbf{r}_1 \ldots d\mathbf{r}_M \tag{9}$$

Going back to equation (6), when $\beta \to 0$ (or M large enough in β/M), we can expect ρ to be significant only when $\mathbf{r}' \simeq \mathbf{r}$: if β/M can be considered small, the operator exponential $\rho(r_i, r_i + 1)$ can be expanded to second order in β/M to yield a gaussian function (a 'broadened' δ function) which Barker [19] introduces:

$$\rho(\mathbf{r}, \mathbf{r}'; \frac{\beta}{M}) = \left(\frac{4\pi}{M}\beta'\right)^{-N/2} \mathrm{e}^{-M\frac{(\mathbf{r}-\mathbf{r}')^2}{4\beta'} - \frac{\beta}{2M}[V(\mathbf{r}) + V(\mathbf{r}')]} \tag{10}$$

where $\beta' = \dfrac{\hbar^2}{2m}\beta$ and N is the number of degrees of freedom. Equations (9) and (10) in practice introduce an effective (dimensionless) potential:

$$V_{\mathrm{eff}}(\mathbf{r}_1 \ldots \mathbf{r}_M) = \sum_i M\frac{(\mathbf{r}_i - \mathbf{r}_{i+1})^2}{4\beta'} - \frac{\beta}{M} V(\mathbf{r}_i) \tag{11}$$

which can be used for simulations.

4.1.2 Simulations.

While Barker [19] uses equation (10) in a Monte-Carlo scheme, one can use the effective potential in equation (11) [20, 21] for molecular dynamics simulations. That potential is then equivalent to that of a ring-polymer (that is, a set of polymers, or necklace of beads, figure 5), each particle being replaced by a set of M beads driven by the effective potential in equation (11). One can thus obtain quantum distributions at finite temperature by e.g. a Langevin dynamics (as briefly outlined in section 4.2.1). It is worth

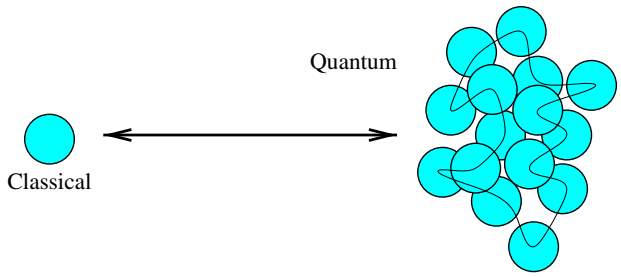

Figure 5. Path integral necklace of beads: each classical particle is replaced by a ring of replicas connected by a harmonic interaction.

pointing out at this stage that, within this formalism, time has in principle no physical meaning.

This formalism has been and is used with success, and has undergone a number of developments [7, 13, 22–25]: its main quality is that, as the number of beads M is increased, the results converge towards the exact quantum solution. This establishes the method as a reference method as its reliability can be thus be controlled. The drawback is the additional computational cost: as M (depending on temperature) can take values up to 50 or more, the computational requirements can skyrocket. Although several methods were devised to reduce these requirements [26–28], work is still restricted to relatively simple and/or small systems.

4.2 The Langevin equation

4.2.1 Background

The Langevin equation was originally devised to describe Brownian motion [29]. It is now currently used for constant-temperature classical molecular dynamics simulations. Indeed, in its generic form, it writes (in 1-D):

$$m\frac{d^2x}{dt^2} = -\frac{dV}{dx} - m\gamma\frac{dx}{dt} + R_T(t) \tag{12}$$

The first term in the right-hand side of equation (12) simply corresponds to Newton's usual equation of motion: acceleration equals force divided by mass. If only this term is retained, the simulation will conserve energy; however, one usually wishes rather to control the temperature of the system as most experiments are carried out at a given temperature.

To control temperature, one thus modifies Newton's dynamics by introducing a temperature dependent random term $R_T(t)$: thermal equilibrium will be reached when the work produced by R_T is compensated for by the dissipative term $-\gamma\, dx/dt$. The fluctuation-dissipation theorem [30] in classical statistical physics imposes that:

$$R_T(t) = \sqrt{2m\gamma k_B T}\varepsilon(t) \tag{13}$$

where $\varepsilon(t)$ is a white noise random variable. Constant γ (a frequency) thus represents the coupling between the system under study and a thermal bath at temperature T. The value of γ is chosen and should, in principle, have no influence on the results provided by the simulation. For that reason, it can be chosen relatively large to ensure rapid relaxation towards thermal equilibrium but when intrinsically dynamical properties are computed (e.g. vibrational spectra) it is usually chosen as small as possible (often a fraction of a THz) which entails slow relaxation towards equilibrium. This choice will therefore result from a compromise.

4.2.2 The Quantum Thermal Bath (QTB)

Several different formalisms were developed [31–33] from these equations to adapt them to quantum systems; the Quantum Thermal Bath (QTB) [33] is probably the simplest and will be detailed below.

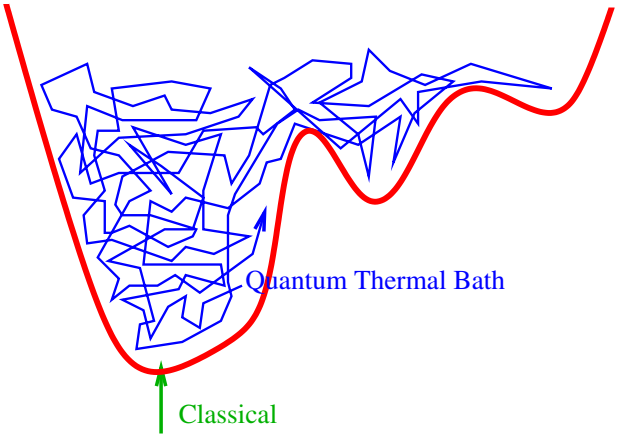

Figure 6. The QTB introduces a stochastic trajectory (blue) to account for quantum delocalization, while a classical particle (green) will remain at the bottom of the potential well (at temperature 0K). The dynamics remains formally classical but produces a quantum correction to the positional distribution.

The Quantum Thermal Bath simply replaces the random term R_T with another random term with a quantum distribution so that it comprises both zero-point energy and thermal effects (figure 6). The stochastic term, provided it is well chosen, will force the particle to move around, mimic quantum delocalization and hopefully generate the correct quantum distributions. In practice, the new probability distribution for the random term is frequency-dependent. Therefore, instead of a 'white' noise (all frequencies have the same weight), a 'colored' (some frequencies weigh more) or correlated in the time domain noise is introduced. This means the spectrum in the frequency domain of R is now the average thermal energy of an harmonic oscillator of angular frequency ω, which writes:

$$\hat{C}^Q_{RR}(\omega) = 2m\gamma\, \Theta^Q_T(\omega) \tag{14}$$

where $\Theta^Q_T(\omega)$ writes:

$$\Theta^Q_T(\omega) = \hbar\omega\left(\frac{1}{2} + \frac{1}{e^{\frac{\hbar\omega}{k_BT}} - 1}\right) \tag{15}$$

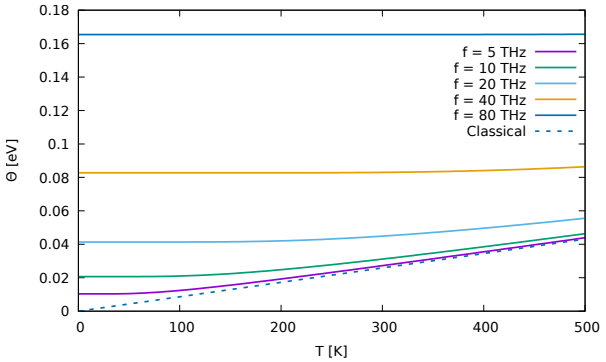

Figure 7. $\Theta_T^Q(\omega)$ (equation (15)) as a function of temperature for several frequencies. The classical counterpart k_BT, which does not depend on frequency, is also shown (dashed line) for comparison.

The sampling obtained from equation (15) is strictly valid only for a harmonic oscillator.

The behavior of $\Theta_T^Q(\omega)$ is shown on figure 7. The classical counterpart is simply k_BT, linear with temperature and non frequency-dependent. Figure 7 clearly shows, firstly, large high-frequency contributions and, secondly, the ZPE contribution at low temperature.

The computational load for the colored random term generation is negligible, so that the QTB involves no significant additional cost with respect to classical simulations. An additional advantage is that it easily allows to compute vibrational spectra which can be compared to, for instance, infra-red absorbtion experiments. Anharmonic features will be enhanced, as they should [34], by the large high-frequency contributions in the random force (see figure 7).

A drawback is that convergence towards the exact quantum distributions cannot be checked as with PI simulations. An ideal procedure, when possible, would therefore be to do short (but expensive) PI simulations to serve as a reference since convergence can be checked, and then run QTB simulations, check the results with those of the PI simulation (and incidentally with known experimental data). Then gather the required data using the capability of the QTB to carry out large simulations and explore several situations, for instance, different isotopes, pressures and temperatures.

4.2.3 Successes...

LiH and LiD.

One of the first successes of the QTB was to account for the different lattice constants and their behavior up to 600K in LiH and LiD [35]: this was done using the QTB associated with force calculations within the DFT. Such isotope effects cannot be accessed classically, as explained in section 3.1.

Pure and salty ice at high-pressure.

The case of high-pressure ice is exposed in section 3.2. NQEs were first pointed out by PI simulations [7], but the QTB [8] confirmed these effects at a much lesser cost and, in addition, provided vibrational spectra that were in excellent accordance with Infra-Red and Raman experiments. The efficiency of the QTB allowed to study and explain the effect of introducing a small amount of different salts (HCl, LiCl and NaCl) [36] with very different behaviors but the same final result: the increase of the VII to X symmetrization transition pressure by 30 GPa.

In Earth's mantle.

It seems that Earth's mantle contains about as much water as the oceans. AlOOH in its δ phase is one of the major vectors thereof. The QTB allowed to establish the quantum-driven transition mechanism to the symmetrized δ' phase [37] at pressures present in the mantle.

4.2.4 And problems: the Zero-Point Energy Leakage (ZPEL) and the adaptive Quantum Thermal Bath (adQTB)

Energy leaks!

Several authors [38–40] have pointed out the contradiction of trying to impose a quantum distribution on a fundamentally classical system. Indeed, Langevin's equation (12) remains a classical equation of motion even when the random term is not a standard white noise. The consequence is that the classical dynamics will tend to distribute energy equally between all degrees of freedom. The QTB pumps more energy at high frequencies than at low frequencies and, due to anharmonic coupling between modes, that excess energy on the high frequency modes tends to flow, or "leak" on to the low energy modes (figure 8). Excessive energy on the low frequency vibrations tends to destabilize the system, alters velocity and positional distributions and eventually will melt the simulated system well below its actual melting temperature. The successes exhibited in section 4.2.3 were mainly obtained at high-pressures that tend to inhibit such dramatic outcomes.

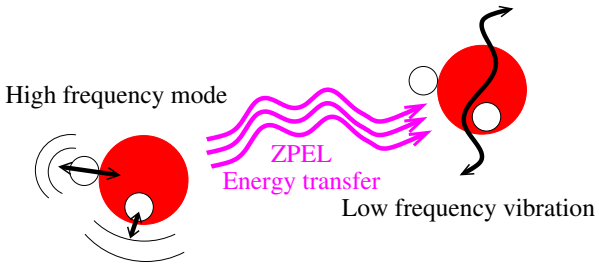

Figure 8. The mechanism of Zero-Point Energy Leakage: the QTB pumps more energy into high frequency modes than into low frequency modes, but the simulation, being classical in practice, will tend to enforce energy equipartition and induce an energy flow from high to low frequency motions. In this this figure the light hydrogen atom (white) vibrate at a high frequency: energy is thus transfered to the low frequency lattice modes mainly involving heavier oxygen (red). This can considerably alter the structure of the system and yield useless results.

The damping coefficient γ in Langevin's equation (12) has the dimension of a frequency, but, as it appears both in the damping and the random terms, it plays the role of a coupling of the system with the thermal bath, whether quantum or not. Strengthening that coupling will force the system closer to quantum distributions, while weakening it will let it remain classical [41]. The choice of that coefficient is therefore not insignificant at all: strong coupling will force the correct distributions but considerably alter the dynamics, as low frequency modes may end up overdamped, weak coupling will let energy pour over low frequency modes and destroy the sample!

A cure must therefore be found, unless it is accepted that only high-pressure studies can be done.

A diagnosis.

The challenge here is to translate Kubo's celebrated fluctuation-dissipation theorem (FDT) [30] into a usable form. Doing this [42] yields that the Fourier transform of the velocity-random force correlation function is related to the Fourier transform of the velocity-velocity correlation function:

$$\mathrm{Re}\left[\hat{C}^{Q}_{vR}(\omega)\right] = m\gamma\,\hat{C}^{Q}_{vv}(\omega) \tag{16}$$

If the FDT holds, the ratio of these two quantities should equal 1. These quantities can easily be computed during a simulation run for all frequencies, and whenever the ratio deviates from 1, ZPEL occurs: a convenient tool for a diagnosis is thus available.

And a cure.

The point now is to enforce equation (16) at all frequencies. Several strategies can be devised: the simplest one is to separate the coupling coefficent γ in Langevin's equation (12) into two parts: firstly, in the actual damping term γ is a constant, but secondly in the random term, the Fourier transform of γ, instead of being a constant becomes frequency-dependent $\hat{\gamma}_R(\omega)$ and can be adapted on-the-fly, for each frequency ω, to enforce equation (16). How well (16) is actually enforced can be monitored to ensure that the adaptation is working properly.

The adaptive-QTB (adQTB) was first tested on a system of Ne_{13} clusters [42] and was proven to prevent the spurious melting of the sample, that the original QTB inevitably produced. An attempt on room-temperature water was also successfully conducted [43] and correctly captured the balance between the quantum-induced strengthening of the hydrogen-bonds by the O−H stretching vibrations and their, also quantum-induced, weakening by the O−H bending modes.

5 Final remarks.

Although the problem of the toxicity of heavy water that was mentioned in the introduction section 1, is not solved in the present paper, the study of NQEs is now entering maturity as practical methods and software exist.

Isotope effects are now of course within reach, but NQEs have many surprises in store for physicists. An example is provided with salty ice at high-pressure [36]: it had been found experimentally [44] that the quantum characteristics of the already mentioned (sect. 3.2) VII-X transition in ice are significantly diminished by the introduction of a small quantity of salt. The initial interpretation was that the introduction of an impurity locally distorts the lattice and therefore inhibits tunneling. QTB simulations introducing NaCl, LiCl or HCl then showed that the cations have very different behaviors: sodium, being relatively bulky, doesn't move much, while lithium migrates to various sites, and hydrogen clings to the nearest oxygen atom..., the transition inhibition remaining exactly the same for the three. Lattice distortion being cation-dependent could not explain such an uniform result. Finally, the realization arose that Na^+Cl^-, Li^+Cl^- and H^+Cl^- all carry the same strong dipolar moment, and that the hydrogen atoms of ice are therefore submitted to, not only the interacton with other water molecules, but also to that dipolar field. That field being slowly decaying with distance has a relatively long range, allowing even a small concentration to make the potential in figures 3 and 4 asymmetric thereore strongly inhibiting tunneling tunneling.

Whenever quantum mechanics is involved, non-intuitive effects arise!

Research is currently pursued both in studying compounds of interest and trying to devise new methods. On the one side, the path integral formulation is devised for the time-independent density matrix, and its extension to time-dependent quantities involves some non straightforward approximations; on the other side, the QTB and its advanced version (the adaptative quantum thermal bath) consider the time evolution of classical quantities under the influence of a bath that reproduces the exact quantum features only for harmonic or mildy anharmonic systems. Time-dependent phenomena thus remain a challenge as the time-dependence of both the QTB (a stochastic process) and the PI (time is rather arbitrary) still is to a large extent an open question [23, 34, 45, 46].

Acknowledgements

The authors gladly acknowledge the work of PhD students Yael Bronstein, Sofiane Schaack, Thomas Plé, Erika Fallacara, Nastassia Mauger, Niccolò Avallone and post-doctoral researcher Étienne Mangaud. They also acknowledge the use of several millions of CPU hours at CINES (Centre Informatique National de l'Enseignement Supérieur).

References

[1] Pyari Mohan Misra, Current Science, **36**, 447-453 (1967)

[2] A. F. Goncharov, V. V. Struzhkin, M. S. Somayazulu, R. J. Hemley, and H. K. Mao, Science **273**, 218 (1996)

[3] K. Aoki, H. Yamawaki, and M. Sakashita, Phys. Rev. Lett. 76, 784 (1996); K. Aoki, H. Yamawaki, M. Sakashita, and H. Fujihisa, Physical Review B **54**, 15673 (1996)

[4] V. V. Struzhkin, A. F. Goncharov, R. J. Hemley, and H. K. Mao, Physical Review Letters **78**, 4446 (1997).

[5] M. Song, H. Yamawaki, H. Fujihisa, M. Sakashita, and K. Aoki, Physical Review B **60**, 12644 (1999).

[6] A. F. Goncharov, V. V. Struzhkin, H. K. Mao, and R. J. Hemley, Phys. Rev. Lett. 83, 1998 (1999).

[7] Magali Benoit, Dominic Marx, and Michele Parrinello, Nature, **392**, 258 (1998).

[8] Yael Bronstein, Philippe Depondt, Fabio Finocchi and Antonino Marco Saitta, Physical Review B, **89**, 214101 (2014)

[9] Erika Fallacara, Philippe Depondt, Simon Huppert, Michele Ceotto and Fabio Finocchi, Journal of Physical Chemistry C **125**, 40, 22328–22334 (2021)

[10] W. R. Busing, Journal of Chemical Physics, **23**, 923 (1955)

[11] I. Kanesaka, M. Tsuchida, and K. Kawai, Journal of Raman Spectroscopy, **13**, 253 (1982)

[12] T. J. Bastow, M. M. Elcombe, C. J. and Howard, Solid State Communications **57**, 339 (1986)

[13] Sofiane Schaack, Étienne Mangaud, Philippe Depondt, Simon Huppert, Erika Fallacara and Fabio Finocchi, *to be published* (2022)

[14] A. Bussmann-Holder, H. Büttner and A. R. Bishop, Journal of Physics: Condensed Matter **12**, L115 (2000)

[15] M. Born and R. Oppenheimer, *Zur Quantentheorie der Molekeln*, Annalen der Physik, **20**, 429 (1927)

[16] P. Hohenberg and W. Kohn, Physical Review **136** B864-B871 (1964)

[17] W. Kohn and L.J. Sham, Physical Review **140** A1133-A1138 (1965)

[18] R. P. Feynman and A. R. Hibbs, *Quantum Mechanics and path integrals*, McGraw-Hill, New York (1965)

[19] J. A. Barker, The Journal of Chemical Physics, **70**, 2914 (1979)

[20] D. Chandler and P. G. Wolynes, The Journal of Chemical Physics, **74**, 7 (1981)

[21] M. Parrinello and A. Rahman, The Journal of Chemical Physics **80**, 860 (1984).

[22] Ceperley, D. M., Rev. Mod. Phys., **67** 2, 279-355, (1995)

[23] I. R. Craig and D. E. Manolopoulos, The Journal of Chemical Physics **121**, 3368 (2004).

[24] B. J. Braams and D. E. Manolopoulos, The Journal of Chemical Physics **125**, 124105 (2006).

[25] Sofiane Schaack, Philippe Depondt, Simon Huppert and Fabio Finocchi, Scientific Reports **10**, 8123 (2020)

[26] Venkat Kapil, Mariana Rossi, Ondrej Marsalek, Riccardo Petraglia, Yair Litman, Thomas Spura, Bingqing Cheng, Alice Cuzzocrea, Robert H. Meißner, David M. Wilkins, Benjamin A. Helfrecht, Przemysław Juda, Sébastien P. Bienvenue, Wei Fang, Jan Kessler, Igor Poltavsky, Steven Vandenbrande, Jelle Wieme, Clemence Corminboeuf, Thomas D. Kühne, David E. Manolopoulos, Thomas E. Markland, Jeremy O. Richardson, Alexandre Tkatchenko, Gareth A. Tribello, Veronique Van Speybroeck and Michele Ceriotti, Computer Physics Communications, **236**, 214-223, (2019)

[27] Fabien Brieuc, Hichem Dammak, Marc Hayoun, Journal of Chemical Theory and Computation, **12**, 3, 1351-1359, (2016)

[28] Michele Ceriotti, David E. Manolopoulos, Michele Parrinello, Journal of Chemical Physics **134**, 084104 (2011)

[29] Paul Langevin, *Sur la théorie du mouvement brownien* [On the theory of brownian motion], Comptes Rendus de l'Académie des Sciences (Paris) **146**, 530–533 (1908).

[30] Ryogo Kubo, Reports on Progress in Physics, **29**, 1, 255, (1966)

[31] Michele Ceriotti, Giovanni Bussi and Michele Parrinello, Physical Review Letters, **103**, 3, 030603 (2009)

[32] Michele Ceriotti, Giovanni Bussi and Michele Parrinello, Physical Review Letters, **102**, 2, 020601 (2009)

[33] Hichem Dammak, Yann Chalopin, Marine Laroche, Marc Hayoun and Jean-Jacques Greffet, Physical Review Letters, **103**, 19,190601 (2009)

[34] Thomas Plé, Simon Huppert, Fabio Finocchi, Philippe Depondt and Sara Bonella, The Journal of Chemical Physics **155**, 104108 (2021)

[35] H. Dammak, E. Antoshchenkova , M. Hayoun, and F. Finocchi, Journal of Physics, Condensed Matter, **24**, 43, 435402, (2012)

[36] Yael Bronstein, Philippe Depondt, Livia E. Bove, Richard Gaal, Antonino Marco Saitta and Fabio Finocchi, Physical Review B, **93**, 2, 024104, (2016)

[37] Yael Bronstein, Philippe Depondt and Fabio Finocchi, European Journal of Mineralogy, **29**, 3, 385-395 (2017)

[38] M. Ben-Nun and R. D. Levine, The Journal of Chemical Physics, **101** 10, 8768–8783, (1994)

[39] Scott Habershon and David E. Manolopoulos, The Journal of Chemical Physics, **131**, 24, 44518(2009)

[40] Raz L. Benson, George Trenins and Stuart C. Althorpe, Faraday Discussions, **221**, 350-366, (2019)

[41] Fabien Brieuc, Yael Bronstein, Hichem Dammak, Philippe Depondt, Fabio Finocchi, Marc Hayoun, Journal of Chemical Theory and Computation, **12**, 5688-5697 (2016)

[42] Étienne Mangaud, Simon Huppert, Thomas Plé, Philippe Depondt, Sara Bonella, Fabio Finocchi, Journal of Chemical Theory and Computation, **15**, 5, 2863–2880, (2019)

[43] Nastasia Mauger, Thomas Plé, Louis Lagardère, Sara Bonella, Étienne Mangaud, Jean-Philip Piquemal and Simon Huppert, Journal of Physical Chemistry Letters, **12** (34), 8285-8291 (2021)

[44] L. E. Bove, R. Gaal, Z. Raza, A. A. Ludl, S. Klotz, A. M. Saitta, A. F. Goncharov, and P. Gillet, Proceedings of the National. Academy of Science USA **112**, 8216 (2015).

[45] J. Cao,J. and G. A. Voth, Journal of Chemical Physics, **99**, 12, 10070-10073, (1993)

[46] J. Cao,J. and G. A. Voth, Journal of Chemical Physics, **100**, 7, 5093-5105 (1994)